MOL # 20701

Bradycardic and proarrhythmic properties of sinus node inhibitors

Juliane Stieber, Karen Wieland, Georg Stöckl, Andreas Ludwig and Franz Hofmann

From the:

Institut für Pharmakologie und Toxikologie der Technischen Universität München,

Biedersteiner Str. 29, 80802 München, Germany.

1

MOL # 20701

Running title: Block of HCN channels results in bradycardia and arrhythmia

Corresponding author:

Juliane Stieber

Institut für Pharmakologie und Toxikologie,

TU München,

Biedersteiner Str. 29,

80802 München, Germany

Tel: 49.89.4140-3286

Fax: 49.89.4140-3261

E mail: stieber@ipt.med.tu-muenchen.de

Text pages: 32

Tables: 1

Figures: 8

References: 30

Words in Abstract: 248

Words in Introduction: 498

Words in Discussion: 1517

Abbreviations: HCN, hyperpolarization-activated, cyclic nucleotide-gated cation channel, HEK, human embryonic kidney cells; i.p. intraperitoneal; 8-Br-cAMP, 8-Bromoadenosine 3',5'-cyclic monophosphate; IC_{50}, half-maximal inhibitory concentration; ED_{50}, half-maximal effective dose;

Abstract

"Sinus node inhibitors" reduce the heart rate presumably by blocking the pacemaker current I_f in the cardiac conduction system. This pacemaker current is carried by four hyperpolarization-activated, cyclic nucleotide-gated cation (HCN) channels. We tested the potential subtype specificity of the sinus node inhibitors cilobradine, ivabradine and zatebradine using cloned HCN channels. All three substances blocked the slow inward current through human HCN1, HCN2, HCN3 and HCN4 channels. There was no subtype-specificity for the steady-state block with mean IC_{50} values of 0.99, 2.25 and 1.96 µM for cilobradine, ivabradine and zatebradine, respectively. Native I_f, recorded from mouse sinoatrial node cells, was slightly more efficiently blocked by cilobradine (IC_{50}: 0.62 µM) than the HCN currents. The block of I_f in sinoatrial node cells resulted in slower and dysrhythmic spontaneous action potentials. The *in vivo* action of these blockers was analyzed using telemetric ECG recordings in mice. Each compound reduced the heart rate dose-dependently from 600 to 200 bpm with ED_{50} values of 1.2, 4.7 and 1.8 mg/kg for cilobradine, ivabradine and zatebradine, respectively. β-adrenergic stimulation or forced physical activity only partly reversed this bradycardia. In addition to bradycardia, all three drugs induced increasing arrhythmia at concentrations above 5 mg/kg for cilobradine, above 10 mg/kg for zatebradine or above 15 mg/kg for ivabradine. This dysrhythmic heart rate is characterized by periodic fluctuations of the duration between the T-wave and P-wave resembling a form of sick sinus syndrome in man. Hence, all available sinus node inhibitors possess an yet unrecognized proarrhythmic potential.

Introduction

The hyperpolarization-activated, cyclic nucleotide-gated cation current termed I_h or I_f is a prominent depolarizing current in a variety of neuronal and cardiac cells that show spontaneous electrical activity (for reviews, see Baruscotti, 2005; Robinson and Siegelbaum 2003). In the heart, this current is especially found in the cardiac conduction system, e.g. in Purkinje fibers and sinoatrial node cells (pacemaker cells) where it is thought to mediate the β-adrenergic stimulation of the heart rate via its direct modulation by cAMP. Four HCN channels underlie the native I_f, with an yet unknown subtype assembly to produce the tissue and cell-specific I_f throughout the organism. In the sinoatrial node, HCN4 is the predominant subtype in all species whereas HCN1, HCN2 and HCN3 are expressed at lower levels and with less specificity for the sinoatrial node compared to the myocardium (Marionneau, 2005). The physiological role of I_f in the adult cardiac conduction system, especially the relevance of I_f for heart rate regulation, has not been fully elucidated to date. HCN2 knockout mice show slight sinus arrhythmia at rest, but in these mice, I_f in sinoatrial cells is only reduced, not eliminated (Ludwig 2003). HCN4 knockout mice die during embryonal development (Stieber 2003b). The heart of these embryos is beating, but at a slow pace which can be attributed to missing pacemaker potentials due to almost completely eliminated I_f in the developing cardiac cells. This, however, does not allow conclusions about the role of I_f/HCN4 in the adult organism. There are no reports about a cardiac phenotype of HCN3 or HCN1 knockout mice. Sinus node inhibitors (SNIs) have been shown to block the native I_f in cells of the cardiac conduction system and in neurons of various species (Bogaert, 1990; Bois, 1996; BoSmith, 1993), even before HCN channels have been identified as the underlying ion channels (Ludwig, 1998; Santoro 1998) and thus as possible targets of sinus node inhibitors. The block of I_f in sheep Purkinje fibers or rabbit sinoatrial node cells results in a slower, or in the case of Purkinje fibers even abolished spontaneous slow depolarization. The slowing effect on

sinoatrial node depolarization has consequently been assumed to be the reason for the bradycardic action of these substances (DiFrancesco and Camm, 2004). For several years, ivabradine, a member of the newer SNIs which also include cilobradine and zatebradine, has been tested in animals (Colin, 2004; Monnet, 2004; Vilaine, 2003; Du, 2004) and humans (Borer, 2003). Interestingly, it has been found, that although this substance has a depressing effect on the heart rate, neuronal side effects are limited to occasional visual symptoms. This led to the clinical development of SNIs as specific bradycardic agents. In addition, SNIs could serve as a tool to study the effects of I_f inhibition specifically in the cardiac conduction system *in vivo*. In this study, we addressed two issues: First, what are the effects of an increasing inhibition of I_f on the mammalian heart rate regulation, and second, are sinus node inhibitors preferably targeting certain HCN subtypes.

MOL # 20701

Material and Methods

Molecular cloning of human HCN channels

Human HCN2 and HCN4 cDNAs were originally cloned from the atrioventricular node region of a human heart (Ludwig, 1999), human HCN1 and HCN3 cDNAs from Whole Human Brain QUICK-Clone cDNA (Clontech, Palo Alto, USA) (Stieber, 2005). All cDNAs were subcloned into the pcDNA3 mammalian expression vector (from Invitrogen, Karlsruhe, Germany).

Functional expression of HCN channels and electrophysiological recordings

Expression of HCN channels in HEK293 cells and voltage clamp experiments were basically done as described (Stieber, 2003a). Briefly, HEK293 cells were transfected with expression vectors encoding one of the human HCN channels using FuGENE6 transfection reagent (Roche, Mannheim, Germany) according to the manufactor's instructions (transfectant/DNA-ratio: 3/1 v/w) or by electroporation using a Biorad system (Biorad, München, Germany) according to the manufactor's instructions. Cells were cultured on polylysated glass coverslips in a modified DMEM complete medium (Quantum 286, PAA Laboratories, Austria) and kept at 37°C, 8.5% CO_2. Currents from transfected cells were recorded with the whole cell patch clamp recording technique at a temperature of 23 ± 1°C. Patch pipettes were pulled from borosilicate glass and had a resistance of 2-5 MΩ when filled with intracellular solution, containing: 10 mM NaCl, 30 mM KCl, 90 mM potassium aspartate, 1 mM $MgSO_4$, 5 mM EGTA, 10 mM HEPES, pH adjusted to 7.4 with KOH. During the recordings, cells were continuously superfused with extracellular (bath) solution, containing: 120 mM NaCl, 20 mM KCl, 1 mM $MgCl_2$, 1.8 mM $CaCl_2$, 10 mM HEPES, 10 mM Glucose, pH adjusted to 7.4 with NaOH. All chemicals for these solutions were obtained from Sigma (Taufkirchen, Germany). Chemical structures of the sinus node inhibitors used are displayed in Figure 1. 10 mM stock

6

solutions (in bidest H_2O) of cilobradine (Boehringer, Biberach, Germany), ivabradine (Institut de Recherches Servier, Suresnes, France), zatebradine (Boehringer, Biberach, Germany) and verapamil (Tocris, Bristol, UK) were stored as aliquots at –20°C for a maximum of four weeks and were diluted into the extracellular solution to the appropriate concentration on the day of the experiment. Application of the drug to the cells was performed by complete exchange of the bath solution with bath solution containing the indicated drug concentration and continuous superfusing. The membrane potential was held at –40 mV. To elicit inward currents, hyperpolarizing steps to –100 mV were repeatedly applied. The protocol used to obtain use-dependent block was as follows (Figure 2A):

1. Drug wash-in period of 10 minutes; cells were clamped at – 40 mV during that time.

2. Repetition of the following activation/deactivation step:

HCN1: -100 mV for 0.5 s/-40 mV for 0.5 s.

HCN2: -100 mV for 2 s/-40 mV for 2 s.

HCN3: -100 mV for 2 s/-40 mV for 2 s.

HCN4: -100 mV for 10 s/-40 mV for 10 s.

The different durations were chosen to account for the different activation/deactivation kinetics of the HCN channels. At the end of the activation pulse, an open probability of 0.5 was reached for each HCN subtype. It is postulated that in this open configuration SNIs are able to bind to the blocking site inside the pore (DiFrancesco and Camm, 2004).

Data were acquired using an Axopatch 200B amplifier and pClamp7 software or a MultiClamp 700A amplifier and pClamp9 software (all Axon Instruments/Molecular Devices, Union City, USA). Analysis was done offline with Origin 6.0. (MicroCal Software, Northampton, USA). HCN current amplitude was defined as the amplitude at the end of the activation pulse minus the amplitude of the initial lag. The first activation after drug wash-in period was taken as baseline, the amplitudes of the subsequent activations were used to calculate the %block at each activation relative to the first activation. Maximal achievable

block for each drug concentration was reached within 30 min. IC_{50} values were obtained by fitting the logarithmically plotted data (%block) with a sigmoidal fit/logistic model: $y=A_2+(A_1-A_2)/(1+(x/x_0)^p)$, where x_0 corresponds to IC_{50}. The Hill coefficient was defined as the slope of this logarithmic fit. Statistical significance was tested by comparing the datasets (%block) for each drug concentration/HCN subtype using the student's-t-test. p-values<0.05 were considered to be significant.

Preparation of sinoatrial node (SAN) cells from murine hearts and electrophysiological recordings

SAN cells for electrophysiological recordings were basically prepared as described (Ludwig, 2003). Briefly, 2-3 months old C57/Bl6 mice were deeply anesthetized with 100 mg/kg ketamine (Ketavet®, Pharmacia & Upjohn GmbH, Erlangen, Germany) and 10 mg/kg xylazine (Rompun®, Bayer AG, Leverkusen, Germany), injected i.p. The beating hearts were quickly removed and placed in prewarmed Tyrode solution containing: 140 mM NaCl, 5.4 mM KCl, 1.8 mM $CaCl_2$, 1 mM $MgCl_2$, 5 mM HEPES and 5.5 mM glucose, pH 7.4. The SAN region between the superior vena cava and the right atrium was excised, minced and placed into modified Tyrode solution containing: 140 mM NaCl, 5.4 mM KCl, 0.2 mM $CaCl_2$, 0.5 mM $MgCl_2$, 1.2 mM KH_2PO_4, 50 mM taurine, 5 mM HEPES and 5.5 mM glucose, pH 6.9. Enzymatic digestion of the tissue was carried out for 30 minutes at 35°C with 1.75 mg/ml collagenase B, 0.4 mg/ml elastase (both Roche, Mannheim, Germany) and 1 mg/ml BSA added to the modified Tyrode solution. After digestion, the modified Tyrode solution was replaced by Storage Solution containing: 25 mM KCl, 80 mM L-glutamic acid, 20 mM taurine, 10 mM KH_2PO_4, 3 mM $MgCl_2$, 10 mM glucose, 10 mM HEPES and 0.5 mM EGTA. The pH was adjusted to 7.4 with KOH. Cells were kept at least 3 hours at 4°C in Storage Solution before they were slowly readapted to calcium containing solutions.

To compare cloned and native channel properties, I_f from SAN cells was recorded in whole cell mode under the same conditions as described above for HCN currents in HEK293 cells, especially at the same bath temperature of $23 \pm 1°C$. The extracellular solution was the same as for recordings from HEK293 cells. The pulse length for repeated activation/deactivation of I_f was 5s/5s. The intracellular solution for measurements on native cells contained: 10 mM NaCl, 130 mM potassium aspartate, 0.04 mM $CaCl_2$, 2 mM Mg-ATP, 6.6 mM creatine-phosphate, 0.1 mM Na-GTP, 10 mM HEPES, pH 7.3. Spontaneous action potentials from SAN cells were recorded at $32 \pm 1°C$ using the perforated patch technique with 200 µM Amphotericin B added to the intracellular solution. Standard AP parameters were calculated as described (Mangoni 2001).

Telemetric ECG-recordings in mice

All animal experiments were performed according to the Guide for the Care and Use of Laboratoy Animals/U.S. National Institute of Health. Male C57/Bl6-mice were housed in single cages in a 12 hour dark-light-cycle environment with free access to food and water. Radiotelemetric ECG transmitters (DSI, St. Paul, USA) were implanted into the peritoneal cavity under general anesthesia with isoflurane/O_2. The ECG leads were sutured subcutaneously onto the upper right chest muscle and the upper left abdominal wall muscle. This resulted approximately in the Lead II position of the ECG electrodes. The animals were allowed to recover for at least 2 weeks before the experiments. Stock solutions of cilobradine (4.5 mg/ml), ivabradine (4.5 mg/ml), zatebradine (4.5 mg/ml) and verapamil (2 mg/ml) were prepared in sterile 0.9% NaCl (Braun AG, Melsungen, Germany), kept at $-20°C$ and diluted with 0.9% NaCl to the desired concentrations in a volume of 100 µl on the day of the experiment. Isoproterenol (Sigma, Taufkirchen, Germany) was dissolved in 0.9% NaCl less than one hour prior to the injection. Data were acquired using the DSI acquisition system. ECG signals were sampled every minute for 20 seconds. After one hour pre-run (unless

otherwise noted), the mice were injected i.p. with the drug. The ECGs were recorded for 3 to 24 hours thereafter. The animals were allowed to recover for at least 48 hours between experiments since the effective half-life (of the SNIs) was up to 12 hours compared to the postulated rather short plasma half-life of only 2 hours (ivabradine/Procoralan®, Dr. R. Derwand, Servier Deutschland GmbH, personal communication). For forced physical activity, animals were trained to run on a custom made, electrically driven treadmill at a speed of approximately 0.4 m/s and 20% ascending slope.

As appropriate, before and after the injection of the drug, ECG parameters, heart rate and heart rate variability were analyzed. The definitions of the ECG intervals are: RR, duration from R to R; PP, duration from P-peak to P-peak; PQ, end of P to beginning of Q; QT, beginning of Q to end of T, where end of T is the return of any T deviation to the isoelectric line; QTc, heart rate-corrected QT interval using the equation $\dfrac{QT}{\sqrt{RR/100}}$ (Mitchell 1998); TP, end of T to beginning of next ECG complex's P. The heart rate in beats per minute was calculated from the RR duration (in ms) as: 60000/RR. The standard deviation of the RR duration (RR-SD) as a measure of heart rate variability was calculated as the standard deviation of the RR durations during a 20 second period. EC_{50} values were obtained by fitting the logarithmically plotted data (heart rate vs. drug concentration) with a sigmoidal fit/logistic model: $y = A_2 + (A_1 - A_2)/(1 + (x/x_0)^p)$, where x_0 corresponds to EC_{50}. On the linear scale, RR values were fitted with an exponential model: $y = A_1 e^{(-x/\tau_1)}$, RR-SD could be fitted with a sigmoidal (Boltzman) model: $y = A_1 + (A_2 - A_1)/(1 + 10^{(\log(x_0) - x)p})$.

Results

Efficient block of all four HCN subtypes by sinus node inhibitors (SNIs)

SNIs are known blockers of I_f. However, since all four subtypes of HCN channels underlie I_f in the heart, we wanted to know if any of the sinus node inhibitors could be used to discriminate between HCN subtypes. The inward currents through all expressed HCN channels were blocked dose- and use-dependently by SNIs at low µM concentrations. For example, 0.01 µM cilobradine did not inhibit current flow through HCN4 channels, whereas 1 µM and 5 µM lead to increasing inhibition (Figure 2B). The development of the inhibition was rather slow. The channels had to be repeatedly activated before the maximal inhibition for the respective drug concentration could be observed. Verapamil, on the other hand, a known calcium channel blocker from which the SNIs have been structurally derived, only induced a small, non-use-dependent block of HCN channels at high concentrations (Figure 2B, lowest panel). Similar to HCN currents, the native I_f of murine sinoatrial node (SAN) cells was blocked efficiently by 5 µM cilobradine (Figure 2C). Again, the block developed rather "slow", since repeated activations were necessary for the block to occur. Comparison of the use-dependent block for all HCN subtypes and I_f (Figure 2D) revealed a difference between the HCN subtypes with respect to the onset of the block. HCN1 and HCN2 channels needed 300 to 500 activations before the steady-state inhibition was reached, whereas HCN3 and HCN4, as well as the I_f were maximally inhibited after 20 to 40 activations. However, the steady-state inhibition reached for each concentration, an important measure for the effectiveness *in vivo*, did not seem to be influenced by this 10-fold difference in use-dependence (Figure 3). The steady-state dose-response curves for HCN1-4 showed no subtype specificity. However, there are differences in the efficiency of the individual SNIs (Table 1). Cilobradine was the most efficient substance with a mean IC_{50} of 0.99 µM, followed by zatebradine (1.97 µM) and ivabradine (2.2 µM). The block of native I_f by

cilobradine was similar efficient with an IC_{50} of 0.62 µM under the same conditions, measured at room temperature (23 ± 1°C). The slope of the dose-response curves was around one for each substance and channel (Table 1) suggesting one docking site per channel.

Cilobradine does not abolish spontaneous action potentials in isolated SAN cells, but changes their shape, frequency and variability

To test the effect of SNIs on action potentials, cilobradine as the most effective HCN channel blocker was chosen. Cilobradine (1 µM) had a prominent effect on spontaneous action potentials, recorded from isolated murine SAN cells (compare Figure 4A and B). The firing frequency was reduced to about half, apparently by prolongation of the duration between action potentials. Statistical analysis of the AP parameters indeed revealed a highly significant prolongation of the cycle lengths from 275±18 ms to 624±154 ms; n=6 (Figure 4C), caused by a slowdown of the diastolic depolarization rate (DDR) from 70±17 mV/s to 21±6 mV/s (Figure 4E). The average maximal diastolic potential (MDP) at the beginning of the pacemaker potential was shifted towards more negative potentials, from –51.7±4.4 mV to –57.6±6.0 mV (Figure 4D). This difference was, however, not significant, possibly due to a high variability of this parameter. The action potential duration, i.e. the duration from reaching the threshold potential at around –40 mV to the return of the potential to the MDP was prolonged from 200±16 ms to 323±33 ms (Figure 4F). This prolongation was caused by a slightly slower repolarization velocity of 0.47 V/s versus 0.62 V/s in the absence of cilobradine (Figure 4G). The slower repolarization velocity contributed only marginally to the slower AP rate. Since impairment of repolarization is caused by a block of repolarizing potassium currents and might cause serious rhythm problems such as Torsades-de-Points arrhythmias, we tested the effect of a high dose of cilobradine (5 µM) on the outward potassium currents of myocytes, isolated from murine atria (data not shown). In agreement to

findings by Goethals (1993), cilobradine induced a small block of the fast activating phase of repolarising potassium currents (from 21 ± 3 pA/pF to 16.4 ± 2 pA/pF at 60 mV, n=12 cells). This reduction was significant at $p<0.05$ and could be responsible for the slightly delayed repolarization. The depolarization (upstroke) velocity, presumably carried by calcium and sodium currents, was not changed significantly by this SNI (0.999 ± 0.05 V/s vs. 0.991 ± 0.08 V/s, data not shown).

Incubation with high concentrations of cilobradine up to 10 µM did not slow the DDR further. However, the cycle lengths (CL) became increasingly variable. Figure 4H shows that 1 µM cilobradine already increased significantly the standard deviation (SD) of the CL. This increasing CL-SD corresponds to the increasing heart rate variability in mice as described below.

SNIs cause bradycardia and arrhythmia in mice

Telemetric ECG recordings in mice allowed the analysis of the heart rate and ECG parameters in response to the application of SNIs in an unrestrained state for the animal. Intraperitoneal injection of cilobradine dose-dependently reduced the heart rate and increased its variability (Figure 5). Identical results were obtained with ivabradine and zatebradine but not with verapamil (Figure 6A). The reduction of the heart rate started at doses of 0.5 mg/kg. The slowest heart rate that could be reached with the SNIs was about 200 bpm. No slower heart rates were reached, even at progressively higher doses. The ED_{50} values for the decrease in heart rate were in a similar range, with cilobradine having the lowest ED_{50} with 1.2 mg/kg, followed by zatebradine (1.8 mg/kg) and ivabradine 4.7 mg/kg) (Table 1). Again, the heart rate was reduced because the R-R interval durations increased in the presence of SNIs (Figure 6B, upper panel), and so did the variability of the R-R intervals, as demonstrated by the increasing standard deviation of the R-R intervals (Figure 6B, lower panel). Doses above 5 mg/kg of the SNIs, however, had an additional effect on the heart rate. They induced a

periodic arrhythmia (Figure 5, lowest panel). This type of arrhythmia started at about 7.5 mg/kg cilobradine, 10 mg/kg zatebradine and 12.5 mg/kg ivabradine. The arrhythmia consisted of a periodic fluctuation of the R-R interval durations (Figure 5, right lowest panel). This periodicity was characterized by cycles in which the P-P intervals got progressively shorter until one whole ECG complex was omitted and the cycle started again with a longer P-P interval (Fig. 7A/B). An AV-conduction block did not seem to be the cause for the arrhythmia since the PQ-intervals showed no abnormal variations during one cycle of arrhythmia (37.9±5.1 ms), and once a P-wave occurred, all following peaks and waves of the ECG complex (Q, R, S, T) were invariably present.

The only interval of the ECG complex that was consistently and in parallel to the P-P interval (Figure 7B) affected by increasing doses of cilobradine was the duration between the end of the T-wave and the beginning of the following P-wave. This TP-interval is basically the diastolic interval and includes the (usually non-visible) slow spontaneous depolarization of the sinus node that leads to the excitation of the atria, visible as P-wave. After injection of saline, 2 mg/kg cilobradine which induces bradycardia and 10 mg/kg cilobradine which induces bradycardia and arrhythmia, the TP duration changed significantly with every dose, from a mean of 47±7 ms (control) to 70±13 ms (2 mg/kg) to 142±38 ms (10 mg/kg) (Figure 7C). Ivabradine and zatebradine had qualitatively the same effects on the ECG parameters as cilobradine only that higher doses were needed in agreement with their higher $ED_{50}s$. SNIs also prolonged the net QT duration, an effect caused by their impact on the heart rate. However, the heart rate-corrected QT durations are not prolonged even at high doses of SNIs (Figure 7C). This result suggested that even though repolarization velocity and repolarizing potassium currents of single cardiac cells are slightly inhibited by a high dose of the drugs (demonstrated for cilobradine, Figure 4), this inhibition does not seem to change significantly repolarization time in the whole animal at reasonable SNI doses.

MOL # 20701

Impaired upregulation of the heart rate after inhibition of I_f

Binding of cAMP to HCN channels has been implicated to participate in the sympathetic upregulation of the beating frequency. To explore the role of I_f in heart rate regulation at stress, we performed two sets of experiments in mice: Pharmacological stimulation with isoproterenol and forced physical activity. Injection of 0.5 mg/kg isoproterenol alone increased the heart rate from a mean of 506±85 bpm to 721±20 bpm within 10 minutes (Figure 8A, C). After about one hour, the heart rate returned to a resting value which was not different from the heart rate after injection of NaCl as a control. Injection of 5 mg/kg cilobradine slowed the heart rate to a mean of 250±42 bpm within 30 minutes, and this effect lasted for over 3 hours. Strikingly, the heart rate after injection of 5 mg/kg cilobradine and, 30 minutes later, 0.5 mg/kg isoproterenol (Figure 8A, lower panel) still increased, but not above a low resting value of 428±15 bpm. Physical activity, like running on a treadmill, increased the heart rate to 744±25 bpm, similar to an isoproterenol injection (Figure 8B, 8C). However, running after an injection of 5 mg/kg cilobradine increased the heart rate only to 442±25 bpm, not further, again similar to the experiment with the pharmacological stimulation. These results indicated that an upregulation of the heart rate under the condition of presumably blocked I_f is still possible, but impaired. Since it was possible that the blocked I_f could be simply unblocked by the binding of cAMP, we tested the effect of cilobradine on cloned HCN channels and native I_f in the absence and presence of cAMP (Figure 8D). Addition of the membrane permeable cAMP analogon 8-Br-cAMP, however, neither increased the steady-state HCN4 current in HEK293 cells nor the sinoatrial I_f after the currents had been blocked by 1 μM cilobradine. These findings suggests that a basic upregulation of the heart rate is independent of I_f, but faster heart rates require I_f.

Discussion

The results of this study can be summarized as follows: 1) Cilobradine, ivabradine and zatebradine block all four HCN channels with the same IC_{50} value and provide no subtype specific blocker. As previously reported for native I_f (Bogaert, 1990; Bucchi, 2002), the block is use-dependent. The use-dependency is affected by the subtype of the channel. 2) Cardiac rhythm in mice is decreased to a basal frequency and can not be further lowered even by supramaximal doses of SNIs. 3) High doses of SNIs induce periodic arrhythmia that has the characteristics of a 2nd degree sinoatrial block. 4) The sympathetic stimulation of the heart rate remains possible but is impaired in the presence of an apparent complete block of I_f by high doses of SNIs.

These findings are in line with previous reports (reviewed in Schram 2002, Satoh 2003, Mangoni 2005) that regulation of the heart rate depends on several independent mechanisms. Our experiments showed that both the normal heart rate and upregulation of the heart rate above resting values require an intact I_f. A characteristic feature of I_f and HCN channels is their direct modulation by cAMP (for reviews, see Baruscotti, 2005; Robinson and Siegelbaum, 2003). Binding of cAMP to HCN4 shifts the voltage dependence of channel opening to more positive values and increases thereby the DDR *in vivo*. However, the persistence of a basic heart rate even when I_f is maximally blocked suggests that I_f is not responsible for the basic pacemaker action potential, supporting notions of other mechanisms for the generation of a slow spontaneous diastolic depolarization independent of I_f, which include the activation of several depolarizing currents ($I_{Ca,T}$, $I_{Ca,L}$, I_{st}, $I_{Na/Ca}$, Ca release from SR) and the inactivation of hyperpolarizing potassium currents. We cannot absolutely rule out that even in the presence of high doses of SNIs, some depolarizing current through HCN channels still flows, because there is always be an equilibrium between blocked and unblocked channels. In contrast to this consideration, an upregulation of the heart rate in the

16

presence of SNIs was only possible from approximately 200 bpm to 450 bpm, not further. This basic upregulation upon sympathetic stimulation is most likely caused by a mechanism that does not involve I_f, but modulation of I_{st} (Mitsuiye 2000), I_{Ca} currents and/or Ca^{2+} release through ryanodine receptors (Satoh, 2003; Mangoni, 2005).

The relation of blocked I_f in the cardiac conduction system and bradycardia has been established and needs no further consideration (Baruscotti, 2005; DiFrancesco and Camm, 2004). However, the induction of very striking dysrhythmias by each tested SNI has not been described before. Although the sinus node inhibitors have been studied both *in vivo* (Borer, 2003; Colin, 2004; Du, 2004; Monnet, 2004; Vilaine, 2003; DiFrancesco and Camm, 2004) and *in vitro* (Goethals, 1993; Bogaert, 2003; DiFrancesco and Camm, 2004), reports of a changed variability of heart rates, AP cycle lengths or diastolic depolarization rates are missing. This lack of information is most likely due to the fact that in these previous studies, the drugs had been applied in a dosage and manner to study only the bradycardic effect of the compounds. In addition, many of the *in vitro* experiments were conducted on Purkinje fibers using electrically triggered action potentials (Bogaert, 2003) which, of course, disguises any spontaneous arrhythmia. We found similar arrhythmias both in the living mouse and – using the most efficient HCN blocker cilobradine - in isolated sinoatrial node cells, pointing to the conclusion that in the whole animal the observed arrhythmia, like the bradycardia, originated in the "leading" pacemaker cell.

Periodic arrhythmias are often associated with Wenckebach's periodicity. Normal Wenckebach's periodicity is typical for a 2nd degree atrioventricular conduction block. In this condition, the AV conduction is impaired, leading to an elongation of the PQ-interval from beat to beat until the interval becomes too long for conduction through the AV node to occur, resulting in one omitted QRS-complex after a P-wave. After that, a new Wenckebach's cycle with a normal PQ-interval starts. In our study, the animals did not show any AV conduction delay. The PQ-intervals did not show unusual variations from beat to beat, and isolated P-

waves without a following QRS complex did not occur. Rather, during one cycle of arrhythmia, the R-R intervals became progressively shorter until one whole ECG complex was left out. This is a sign for a 2nd degree sinoatrial block, sometimes called "SA (sinoatrial)-Wenckebach's" periodicity. In accordance to this, the only ECG-interval that was affected by SNIs was the TP duration which represents the diastolic phase in which the sinoatrial excitation builds up, eventually leading to the excitation of the atria, visible as the P-wave.

With the data available to date, we propose two basic mechanisms that, likely in combination, could underlie this periodic disturbance of sinus node excitation after application of SNIs. First, inhibition of I_f has different effects on individual sino-atrial node cells since the sinus node is a heterogeneous structure. The cells in the center are postulated to function as leading pacemaker cells. Ion channel density including I_f increases from center to periphery (reviewed in Kodama 2004), and so does conduction velocity. Paradoxically, the AP rate in the intact sinus node is highest in the center, complying with the function as leading pacemaking site, but in *isolated* cells from the sinus node, the AP rate is higher in cells from the periphery. SNIs could have a stronger impact on the leading pacemaker cells with their smaller current density. Eventually, they fire too slow, so cells from the periphery initiate the next beat. Without the depolarizations and regulations from the center, their firing rate gets faster and faster until nonpacemaking atrial cells interfere or excitation-refractory is reached, causing the pause. Then a slower pacemaker cell in the center can take over again. Second, the arrhythmia could arise in one leading pacemaker cell because SNIs have been shown to block I_k and $I_{Ca,L}$ (but, e.g., not $I_{Ca,T}$) at high concentrations in addition to I_f in SAN cells (Goethals 1993, DiFrancesco 2004). The block of these currents was not very effective: 10 µM zatebradine or ivabradine blocked I_K by 18% and 16%, respectively, and $I_{Ca,L}$ by 7% and 18%, respectively. But still, this could lead to an imbalance of the ionic mechanisms usually working together in pacemaking: The block of depolarizing currents (I_f and $I_{Ca,L}$) in sinoatrial node cells, or of the repolarizing I_K in the myocardium, would result in a slower AP-rate, but the block of the

18

outward I_K in sinoatrial node cells, on the other hand, would tend to accelerate the diastolic depolarisation by keeping the membrane potential closer to the AP threshold potential. Depending on the degree of block of the individual currents, this results only in bradycardia or additional arrhythmia.

Since a large I_f is present in other parts of the cardiac conduction system as well, the question might arise, why inhibition of this current does not influence conduction. Most likely, I_f has no influence on triggered action potentials. Although Purkinje fibers have a certain potential for spontaneous depolarizations, this activity is normally overridden by the oncoming depolarizations from faster firing cells. On the other hand, the inhibition of I_f in the whole cardiac conduction system may be the reason for the lack of escape rhythms even though no excitation of the sinus node was sometimes observed for several seconds (corresponding to up to 40 heart beats in the mouse) during the arrhythmias.

We did find slight subtype-specific differences in the use-dependent onset of the block, even when, in the case of HCN2 and HCN3, the same activation/deactivation times and thus exposure times to the drugs, were used. This is in accordance with available data from other groups. The block of I_f by cilobradine in sheep Purkinje fibers (Bogaert, 2003) or mouse sinoatrial node cells in our experiments, or by ivabradine in rabbit sinoatrial node cells (Bucchi, 2002) was completed after 40 activations, whereas 150-200 activations were required to block the I_h recorded from mouse dorsal root ganglion neurons (Raes, 1998). Assuming HCN4 to be the major HCN subtype of I_f in the cardiac conduction system and HCN1 and HCN2 to be the major neuronal subtypes, the data match, even though the molecular basis for this remains to be documented.

To study the effect of I_f inhibition *in vivo*, the time to onset of action might be less important than the steady state inhibition. There were no differences in the steady-state inhibition between the HCN subtypes, although the three used SNIs differed slightly in their IC_{50} values. Cilobradine was the most effective HCN current blocker, followed by zatebradine and

ivabradine. This order of efficiency is very interesting since it is exactly the order determined for both the induction of bradycardia and arrhythmia *in vivo*. This similarity suggests that both conditions are primarily caused by an increasing block of HCN channels despite the potential involvement of other ionic mechanism discussed above.

In conclusion, SNIs cause bradycardia and arrhythmia primarily by inhibition of I_f which impairs the slow diastolic depolarization of sinoatrial pacemaker cells. The major physiological role of I_f seems to be its contribution to the pacemaker potential at fast heart rates.

References

Baruscotti M, Bucchi A, DiFrancesco F (2005) Physiology and pharmacology of the cardiac pacemaker ("funny") current. *Pharmacology & Therapeutics* 107: 59-79.

Bogaert PP, Goethals M, Simoens C (1990) Use- and frequency-dependent blockade by UL-FS 49 of the I_f pacemaker current in sheep cardiac Purkinje fibres. *Eur J Pharmacol* 187: 241-256.

Bogaert PP and Pittoors F (2003) Use-dependent blockade of cardiac pacemaker current (I_f) by cilobradine and zatebradine. *Eur J Pharmacol* 478: 161-171.

Bois P, Bescond J, Renaudon B, Lenfant J (1996) Mode of action of bradycardic agent, S 16257, on ionic currents of rabbit sinoatrial node cells. *Br J Pharmacol* 118: 1051-1057.

BoSmith RE, Briggs I, Sturgess NC (1993) Inhibitory actions of ZENECA ZD7288 on whole-cell hyperpolarization activated inward current (I_f) in guinea-pig dissociated sinoatrial node cells. *Br J Pharmacol* 110: 343-349.

Borer JS, Fox K, Jaillon P, Lerebours G (2003) Antiangial and antiischemic effects of ivabradine, an I_f inhibitor, in stable angina. *Circulation* 107: 817-823.

Bucchi A, Baruscotti M, DiFrancesco D (2002) Current-dependent block of rabbit sino-atrial node I_f channels by Ivabradine. *Journal of General Physiology* 120: 1-13.

Colin P, Ghaleh B, Monnet X, Hittinger L, Berdeaux A (2004) Effect of graded heart rate reduction with ivabradine on myocardial oxygen consumption and diastolic time in exercising dogs. *J Pharmacol Exp Ther* 308: 236-240.

DiFrancesco D, Camm JA (2004) Heart rate lowering by specific and selective I_f current inhibition with ivabradine. *Drugs* 64: 1757-65.

Du XJ, Feng X, Gao XM, Tan TP, Kiriazis H, Dart AM (2004) I_f channel inhibitor ivabradine lowers heart rate in mice with enhanced sympathoadrenergic activities. *Br J Pharmacol* 142(1): 107-12.

Goethals M, Raes A, Bogaert PP (1993) Use-dependent block of the pacemaker current I_f in rabbit sinoatrial node cells by Zatebradine (UL-FS 49). *Circulation* 88: 2389-2401.

Kodama I, Honjo H, Dobrzynski H, Boyett M (2004) Cellular mechanisms of sinoatrial activity, in: *Cardiac Electrophysiology. From Cell to Bedside* (Zipes DP and Jalife J eds) pp 192-202, Saunders/Elsevier Inc., Philadelphia.

Ludwig A, Zong XG, Jeglitsch M, Hofmann F, Biel M (1998) A family of hyperpolarization-activated mammalian cation channels. *Nature* 393: 587-591.

Ludwig, A., Zong, X, Stieber, J., Hullin, R., Hofmann, F., Biel, M. (1999) Two pacemaker channels from human heart with profoundly different activation kinetics. *EMBO J* 18(9): 2323-2329.

MOL # 20701

Ludwig A, Budde T, Stieber J, Moosmang S, Wahl C, Holthoff K, Langebartels A, Wotjak C, Munsch T, Zong XG, Feil S, Feil R, Lancel M, Chien KR, Konnerth A, Pape, HC, Biel M, Hofmann F. (2003) Absence epilepsy and sinus dysrhythmia in mice lacking the pacemaker channel HCN2. *EMBO J* 22: 216-224.

Mangoni ME, Nargeot N (2001) Properties of the hyperpolarization-activated current (I_f) in isolated mouse sino-atrial cells. *Cardiovasc Res* 52: 51-64.

Mangoni, ME, Couette B, Marger L, Bourinet E, Striessnig J, Nargeot J (2005) Voltage-dependent calcium channels and cardiac pacemaker activity: From ionic currents to genes. *Progress in Biophysics and Molecular Biology*, Jun 22 (Epub ahead of print).

Marionneau C, Couette B, Liu J, Li H, Mangoni ME, Nargeot J, Lei M, Escande D, Demolombe S (2005) Specific pattern of ionic channel gene expression associated with pacemaker activity in the mouse heart. *J Physiol (Lond)* 562.1: 223-234.

Mitsuiye T, Shinagawa Y, Noma A (2000) Sustained inward current during pacemaker depolarization in mammalian sinoatrial node cells. *Circ Res* 87: 88-91.

Mitchell GF, Jeron A, Koren G (1998) Measurement of heart rate and Q-T interval in the concious mouse. *Am J Physiol* 274: H747-51.

Monnet X, Colin P, Ghaleh B, Hittinger L, Giudecelli J-F, Berdeaux A (2004) Heart rate reduction during exercise-induced myocardial ischaemia and stunning. *European Heart Journal* 25: 579-586.

Raes A, Van de Vijver G, Goethals M, Bogaert PP (1998) Use-dependent block of I_h in mouse dorsal root ganglion neurons by sinus node inhibitors. *Br J Pharmacol* 125: 741-750.

Robinson RB, Siegelbaum SA (2003) Hyperpolarization-activated cation currents: From molecules to physiological function. *Annu. Rev. Physiol* 65: 453-80.

Santoro B, Liu D, Yao H, Bartsch D, Kandel ER, Siegelbaum SA, Tibbs GR (1998) Identification of a gene encoding a hyperpolarization-activated pacemaker channel of brain. *Cell* 93: 717-729.

Satoh H (2003) Sino-atrial nodal cells of mammalian hearts: Ionic currents and gene expression of pacemaker ionic channels. *J Smooth Muscle Res* 39: 175-193.

Schram G, Pourrier M, Melnyk P, Nattel S (2002) Differential distribution of cardiac ion channel expression as a basis for regional specialization in electrical function. *Circ Res* 90: 939-950.

Stieber J, Thomer A, Much B, Schneider A, Biel M, Hofmann F (2003a) Molecular basis for the different activation kinetics of the pacemaker channels HCN2 and HCN4. *J Biol Chem* 278: 33672-80.

Stieber J, Herrmann S, Feil S, Löster J, Feil R, Biel M, Hofmann F, Ludwig A (2003b) The hyperpolarization-activated channel HCN4 is required for the generation of pacemaker action potentials in the embryonic heart. *PNAS* 100: 15235-40.

MOL # 20701

Stieber J, Stöckl G, Herrmann S, Hassfurth B, Hofmann F (2005) Functional expression of the human HCN3 channel. *J Biol Chem* 280: 34635-34643.

Vilaine JP, Bidouard JP, Lesage L, Reure H, Peglion JL (2003) Anti-ischemic effects of ivabradine, a selective heart rate-reducing agent, in exercise-induced myocardial ischemia in pigs. *J Cardiovasc Pharmacol* 42: 688-96.

MOL # 20701

Footnotes

Unnumbered Footnote:

Name and address for reprint requests: Juliane Stieber, Institut für Pharmakologie, TU

München, Biedersteiner Str. 29, 80802 München, Germany; stieber@ipt.med.tu-

muenchen.de.

Figure legends

Figure 1

Chemical structures and molecular weights (MW) of the SNIs cilobradine (DK-AH269), ivabradine (S16257-2) and zatebradine (UL-FS49), and the related calcium channel blocker verapamil. All substances in this study have been used as hydrochloride salts.

Figure 2

Use-dependent block of HCN currents and native I_f. *A*, pulse protocol for the voltage clamp measurements of HCN channels, expressed in HEK293 cells and I_f, recorded from isolated mouse sinoatrial node cells. Duration of activation/deactivation depends on HCN subtype, please refer to Material and Methods. *B*, example of use-dependent block of cloned HCN channels, shown for HCN4 in the presence of three concentrations of cilobradine. Inward currents were elicited by applying the pulse protocol described in A. Different cells were used for each measurement. "*number*x" in the graphics refers to number of activation at which the current trace was elicited after application of the drug. No block was obtained with 0.01 µM cilobradine after 50 activations whereas with 5 µM cilobradine, maximum block was achieved with less than 50 activations. In comparison, 50 µM verapamil only induced a small, instant block of HCN4 channels. *C*, block of native I_f by 5 µM cilobradine. Maximum block for this concentration was achieved after 20 activations. *D*, comparison of use-dependent block of HCN1, HCN2, HCN3 and HCN4 channels, as well as the native I_f by 5 µM cilobradine. All currents are blocked to the same extent but only 20-40 activations are required for HCN3, HCN4 and I_f to reach this block whereas 300-500 activations are required

MOL # 20701

for HCN1 and HCN2. Values are mean ± sem, n = 4-9 for each current in this graphic.

Meaning of symbols are: squares: HCN1, circles: HCN2, triangles: HCN3, diamonds: HCN4,

stars: I_f.

Figure 3

Steady-state inhibition of HCN1, HCN2, HCN3 and HCN4 channels by cilobradine, ivabradine and zatebradine as well as the inhibition of sinoatrial I_f by cilobradine. Values are mean inhibition ± sd of currents at the indicated drug concentration determined after 500 activations for HCN1 and HCN2, after 50 activations for HCN3 and HCN4 and after 30 activations for I_f. n-numbers used to establish the curves are given in Table 1. Superimposed dose-response curves represent logistic fits of means. Meaning of symbols are (for all three panels): Square/short-dotted line: HCN1; circle/dash-dotted line: HCN2; triangle/dotted line: HCN3, diamond/dashed line: HCN4, open stars, solid line: I_f.

Figure 4

Effect of 1 µM cilobradine on spontaneous action potentials (AP) recorded from isolated murine sinoatrial node cells at 32°C. *A*, example of APs recorded from the same cell before and *B*, 60 s after application of the SNI. Parameters shown in C-H are depicted in B. C-H, comparison of cycle length CL (C), maximal diastolic potential MDP (D), diastolic depolarization rate DDR (E), action potential duration APD (F), repolarization velocity V_{Rep} (G) and standard deviation of cycle length CL-SD (H) of APs recorded before ("bath") and after ("cilobradine") drug application. Values are mean ± sd, n=6. ***p<0.001. Of the AP

parameters, all except MDP differ significantly before and after the application of cilobradine.

The increase in CL-SD (H) indicates increasing AP arrhythmia in the presence of the SNI.

Figure 5

Examples of telemetric ECG recordings in freely moving mice after injection of a SNI.

Left panels: Recordings from a mouse 30 minutes after i.p. injection with saline, 2 mg/kg, 5

mg/kg or 10 mg/kg cilobradine. *Right panels* display the corresponding R to R interval

durations obtained by peak-to-peak analysis of the ECG complexes. 2 and 5 mg/kg

cilobradine induce increasing bradycardia without abnormal arrhythmia, 10 mg/kg cilobradine

induces bradycardia and arrhythmia characterized by periodic fluctuations of the R-R

durations.

Figure 6

Dose-dependent heart rate reduction and arrhythmia induction in mice by SNIs. *A*,

Heart rates in beats per minute 30 minutes after i.p. injection of cilobradine, ivabradine and

zatebradine of the indicated doses. Symbols represent mean ± sd, superimposed dose-response

curves represent logistic fits of the means. Mean heart rates after injection of verapamil is also

given but no fit since verapamil did not affect the heart rate at doses comparable to the SNIs.

n=6-10 mice per dose and drug (also given in Table 1). The ED_{50} of ivabradine differs

significantly at $p<0.001$ from both cilobradine and zatebradine. ***B, upper panel***: R-R intervals

and ***B, lower panel***: the R-R standard deviation from beat to beat as a means to describe

arrhythmia after injection of indicated doses of the drugs. All drugs induce arrhythmia at

doses above 5 mg/kg with ivabradine requiring the highest and cilobradine the lowest dose for the arrhythmia to appear. Symbols represent mean ± sem, fits represent exponential fit in upper panel and sigmoidal fit in lower panel, with: circles/solid line: cilobradine; diamonds/dash-dotted line: zatebradine; squares/dotted line: ivabradine. Note linear scales, n-numbers are the same as in A.

Figure 7

Effects of SNIs on the cardiac electrical activity in mice. *A,* enlarged ECG examples from Figure 5, bottom panel, showing one cycle of the typical arrhythmia caused by a high dose of the SNI cilobradine. P, Q and end of T (here: return of negative part of T deviation to isoelectric line) from which the parameteres in *B* were calculated, are indicated in the lower enlargement. *B,* PP, TP and PQ durations corresponding to the ECG stretch displayed in A, upper panel. The duration of the PP-interval decreases with each heart beat until a pause occurs. This fluctuation in PP durations is independent of the PQ durations but caused by equally varying TP durations. *C*, statistical analysis of the TP-, PQ-, QT- and QTc durations. n = 6 mice, with analysis performed on a 20-second ECG-stretch per animal, before ("unmodulated") and after application of 2 or 10 mg/kg of the drug. The TP duration is highly significantly prolonged by SNIs and fluctuations in the TP duration are responsible for the arrhythmia. SNIs also prolong the QT duration significantly, but the heart rate corrected QTc duration is not significantly different. $*p< 0.05$, $***p<0.001$.

Figure 8

Reduced sympathetic upregulation of the heart rate in mice after application of a SNI.

A, Time course of heart rate after i.p. injection of cilobradine and isoproterenol (β-adrenergic stimulation). *A, upper panel*: Heart rate after the injection of 100 µl 0.9% NaCl as control ("NaCl",dotted line), 5 mg/kg cilobradine ("Cilo", solid line) or 0.5 mg/kg isoproterenol ("Iso", dash-dotted line). Injection was done at time point 0 (vertical line). *A, lower panel*: Heart rate after cilobradine/isoproterenol injection. 5 mg/kg cilobradine was injected at t=0 (first vertical line), 0.5 mg/kg isoproterenol was injected 30 minutes after cilobradine (second vertical line). The β-adrenergic stimulation was only able to increase the heart rate from bradycardia (about 250 bpm) to a low-resting level of about 450 bpm, compared to up to 750 bpm after the injection of isoproterenol without cilobradine. n=6 mice for each experiment, each experiment was done twice. Values are mean ± sd. *B*, Heart rate before, during and after a 10 minute run on a treadmill, *B, upper panel*: without, and *B, lower panel*: with injection of 5 mg/kg cilobradine before the run. Similar to the drug-induced β-adrenergic stimulation, the SNI prevents upregulation of the heart rate above a low-resting level. *C*, Statistical analysis of the heart rate modulations shown in A and B. For this analysis, the heart rate reached 30 minutes after the injection at t=0 (A, upper panel) or after the second injection (A, lower panel) or the maximum reached during the run (B) was taken. Levels of significance are indicated: Dash-dotted lines/*: $p<0.05$; Solid lines/**: $p<0.01$; dashed lines/***: $p<0.001$. *D*, HCN currents or I_f, blocked by cilobradine, cannot be "unblocked" by cAMP. Partial block of HCN4 channels (left side of graphic) or I_f (right side of graphic) by 1 µM cilobradine was obtained by repeated activation steps to –100 mV as described in Figure 2 and is given as residual current from unmodulated currents which are set to 100%. In the presence of 1 µM cilobradine, 100 µM 8-Br-cAMP was then added to the bath solution while inward currents were continuously elicited by steps to – 100 mV.

Table 1

Effects of sinus node inhibitors on HCN channels, I_f in sinoatrial node cells and *in vivo*.

Half-maximal inhibitory concentrations (IC_{50}) and slopes of logistic fit (Hill coefficient) of the dose-response curves displayed in Figure 3 for cilobradine, ivabradine and zatebradine on expressed HCN channels. In addition, the IC_{50} for cilobradine on native I_f recorded from isolated mouse sinoatrial node cells has been determined. Half-maximal effective doses (ED_{50}) for the three drugs have been determined by analyzing the bradycardic effect in mice (Fig. 6A). Numbers in brackets give the number of mice/cells used to establish the dose-response curves.

HCN subtype	IC_{50} (µM)	Hill coefficient	ED_{50}
Cilobradine (10 animals)			*1.2 mg/kg*
HCN1 (33)	1.15 ± 0.16	1.3 ± 0.24	
HCN2 (42)	0.90 ± 0.07	1.3 ± 0.13	
HCN3 (37)	0.99 ± 0.16	1.1 ± 0.18	
HCN4 (37)	0.92 ± 0.05	1.2 ± 0.09	
I_f (28)	0.62 ± 0.18	0.8 ± 0.22	
Ivabradine (6 animals)			*4.7 mg/kg*
HCN1 (56)	2.05 ± 0.13	1.9 ± 0.19	
HCN2 (27)	2.29 ± 0.13	1.6 ± 0.12	
HCN3 (38)	2.51 ± 0.13	1.3 ± 0.07	
HCN4 (17)	2.15 ± 0.34	1.3 ± 0.22	
Zatebradine (10 animals)			*1.8 mg/kg*
HCN1 (27)	1.83 ± 0.39	1.2 ± 0.22	
HCN2 (26)	2.21 ± 0.21	1.1 ± 0.08	
HCN3 (24)	1.90 ± 0.13	1.1 ± 0.08	
HCN4 (22)	1.88 ± 0.12	1.2 ± 0.06	

Cilobradine
MW: 519.1

Ivabradine
MW: 507.0

Zatebradine
MW: 529.5

Verapamil
MW: 491.1
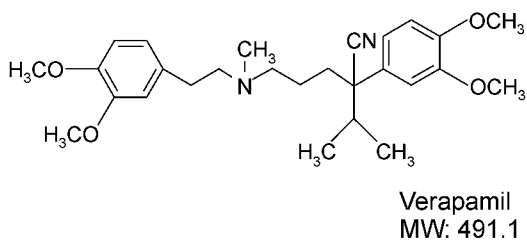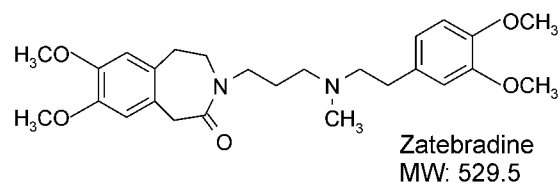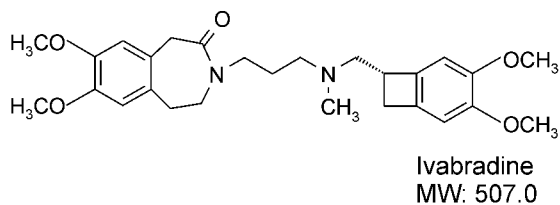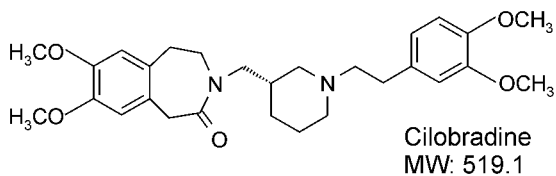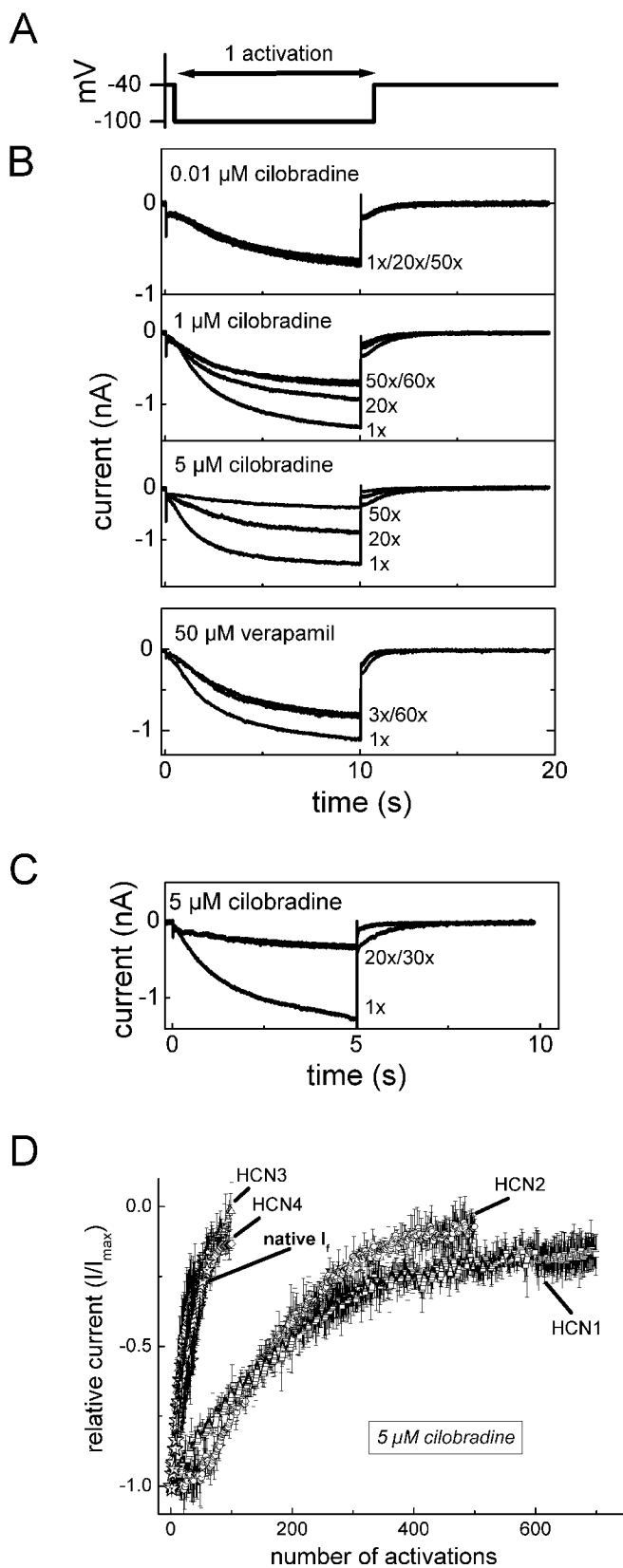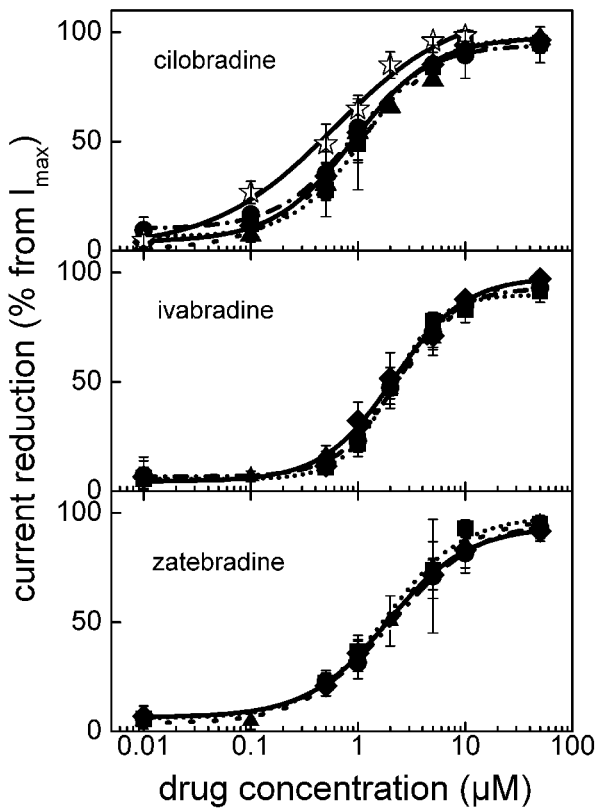
Figure 1

Figure 2

Figure 3
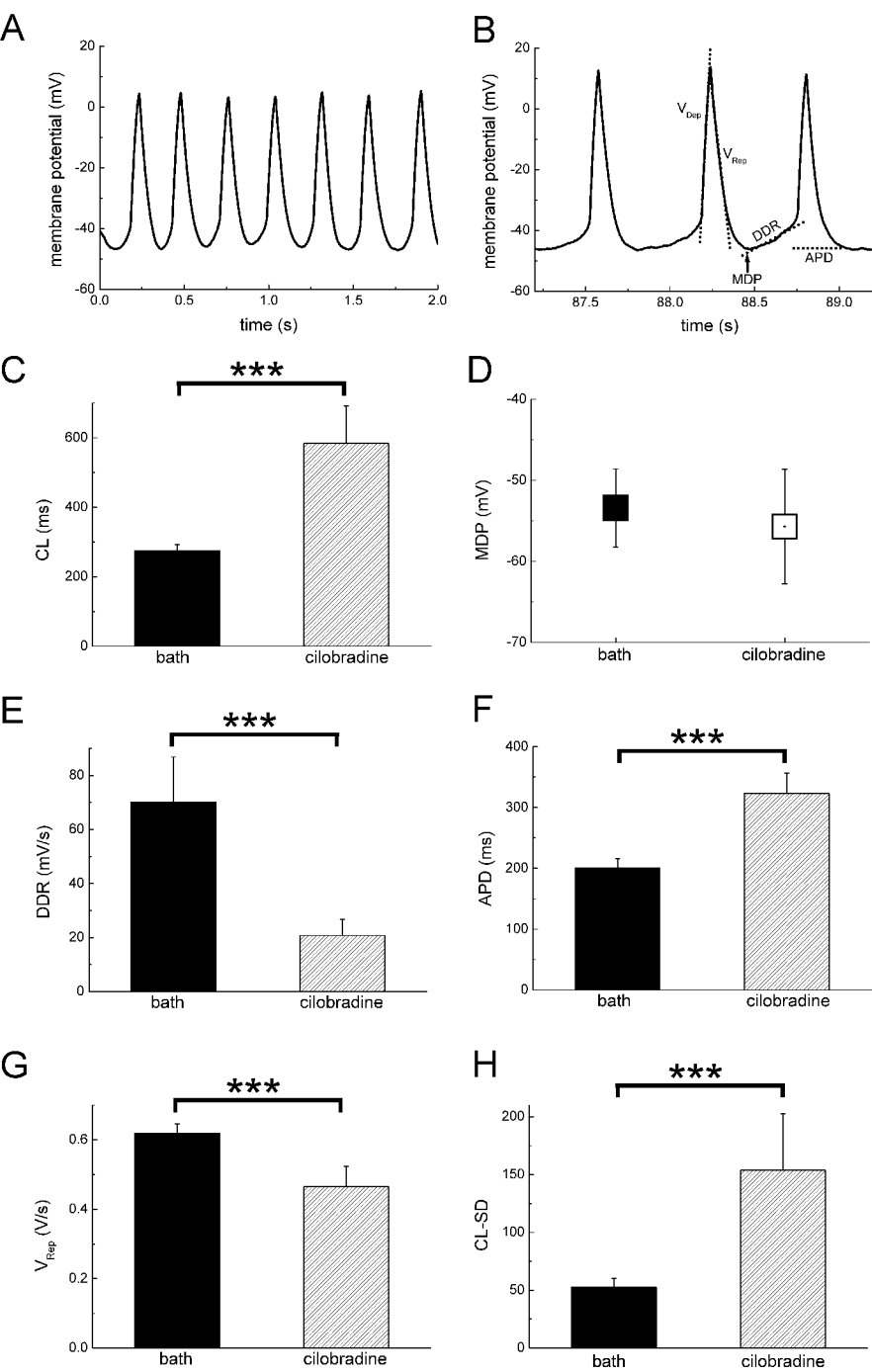
Figure 4

Figure 5

A

B

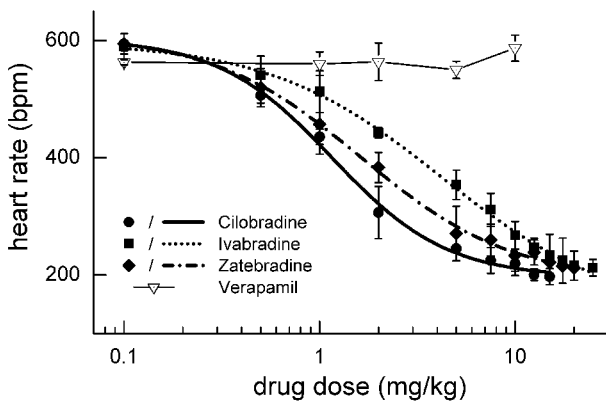Figure 6

A

1 s

P   P   P   end of T   P   end of T   P

Q   Q   Q   Q   Q

B

- PP-interval
- TP-interval
- PQ-interval

duration (s)

#of ECG-complex (in 7A, upper panel)

C

Q-T

P-Q   T-P

- unmodulated
- 2 mg/kg Cilobradine
- 10 mg/kg Cilobradine

duration (s)

***

*   ***

P-Q   Q-T   QTc   T-P

Figure 7

Figure 8